Molecular BioSystems

Accepted Manuscript

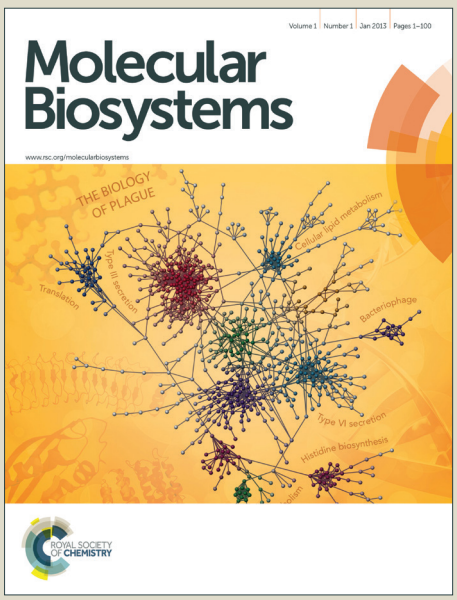

ROYAL SOCIETY OF CHEMISTRY

www.rsc.org/molecularbiosystems

Elementary mode analysis reveals that *Clostridium acetobutylicum* modulates its metabolic strategy under external stress

Manish Kumar[1], Supreet Saini[2,*], and, Kalyan Gayen[3,*]

[1] Department of Chemical Engineering, Indian Institute of Technology Gandhinagar, Ahmedabad - 382424, India

[2] Department of Chemical Engineering, Indian Institute of Technology Bombay, Powai, Mumbai - 400076, India

[3] Department of Chemical Engineering, National Institute of Technology Agartala, Tripura - 799053, India

* Corresponding Authors. Email: saini@che.iitb.ac.in (SS), kalyan.chemical@nita.ac.in (KG).Phone: 91 22 2576 7216 (SS), 913812346630 (KG). Fax: 91 22 2572 6895 (SS), 913812346360 (KG)

Abstract

Clostridium acetobutylicum is a strict anaerobe which exhibits two distinct steps in its metabolic network. In the first step, sugars are oxidized to organic acids (acetic and butyric). This is accompanied with growth. The acids produced in the first phase are re-assimilated into solvents (acetone, butanol, and ethanol) in the second phase of metabolism. The two phases are hence called acidogenesis and solventogenesis, respectively. In this work, using Elementary Mode Analysis (EMA), we quantify fluxes through Elementary Modes in different physical and chemical conditions. Our analysis reveals that, in response to external stresses, the organism invokes Elementary Modes which couple acidogenesis and solventogenesis. This coupling leads to the organism exhibiting characteristics of both, acidogenesis and solventogenesis at the same time. Significantly, this coupling was not invoked during any "unstressed" condition tested in this study. Overall, our work highlights the flexibility in the *Clostridium acetobutylicum* to modulate its metabolism to enhance chances of survival in harsh conditions.

Key words: *Clostridium acetobutylicum*; Elementary Mode Analysis; Biofuel; Acidogenesis; Solventogenesis

Introduction

Clostridium acetobutylicum (*C. acetobutylicum*) is a strict anaerobic, gram-positive bacterium which yields organic solvents as part of its fermentation end products[1,2]. Primary among these products are the solvents acetone, butanol, and ethanol - and hence, the metabolism of the organism is collectively referred to as ABE fermentation[3]. Metabolism in *Clostridium* consists of two distinct phases. In the first phase, a carbon source (such as glucose) is oxidized to organic acids (acetic and butyric acid). This is accompanied with growth and a drop in media pH. Upon accumulation of acids beyond a critical level and in response to cellular and environmental cues, the bacterium enters the second phase of the metabolism[4]. In the second phase, the acids produced in the first phase are assimilated to yield acetone, butanol, and ethanol. The two phases are referred to as acidogenesis and solventogenesis, respectively. A characteristic feature of solventogenesis is the absence of growth[5,6]. While the metabolic reactions and the associated genes are well characterized, very little is known about the dynamic regulation of the switch from acidogenesis to solventogenesis in the metabolic network, which makes it difficult to engineer strains with enhanced solvent yields[7–9]. In addition, mechanism based modeling is further restricted by limited knowledge about the kinetic parameters involved in the reactions and the link between metabolism and sporulation[10–13].

In contrast, constraint-based modeling approaches, which require only physiochemical constraints such as stoichiometry, topology of the network, and the directionality of reactions, have potential for phenotypic characterization of metabolic network through quantification of flux distribution[14,12]. Recent developments such as reconstruction and in vivo experimental studies have revealed new insights towards complementing annotations of few incomplete pathways in genome, such as pentose phosphate pathway and citric acid cycle[15–19]. These developments have led to an alternate framework to analyze the network through flux distribution.

Elementary Mode Analysis (EMA), a constraint-based approach, has been used for studying metabolic network of a number of organisms[20,14,9,21–26]. An elementary mode is defined as a possible sub-pathway, which has a minimal set of enzymes that can operate at the steady state (with irreversible reactions in network)[27–29]. In this approach, a network is first converted into smaller elementary modes. These elementary modes, in turn, are used to quantify flux

through individual reactions using matrix algebra[30,12,28,31,32]. Software tools such as CellAnalyzer[33], YANA, and YANAsquare[34,35] are publicly available for generating elementary modes from metabolic networks.

In this work, we employ EMA to answer the following question: how does *C. acetobutylicum* modulate its metabolic fluxes in response to changes in environmental conditions? In other words, how does the metabolic network aid survival and growth? Using Elementary Mode Analysis, we demonstrate that the organism is able to modulate the carbon fluxes and activate specific elementary modes which are otherwise inactive. Interestingly, this modulation is limited to conditions where the bacterium is subjected to an external stress. By external stress, we mean any addition/removal of a cue by an agent other than *C. acetobutylicum* and hence differentiate it from the acid/solvent stress on the bacterium resulting from fermentation in the organism itself. More specifically, in conditions of stress, the organism invokes elementary modes in solventogenesis phase which couple growth with solvent production. We speculate that this flexibility in the metabolic fluxes in *C. acetobutylicum* aids the bacterium change its metabolic strategy in response to presence of competitors or changes in physical environment. This is likely to aid survival, and potentially outlast its competitors.

Methods and materials

Mathematical method

Biochemical reactions in *C. acetobutylicum*'s metabolic network were obtained from KEGG (Kyoto Encyclopedia of Genes and Genomes) database (Supplementary file 1, Table S2)[15,36,16,17,37]. A METATOOL integrated software tool, YANAsquare developed by Schwarz et al.[34] was employed to generate Elementary Modes (EMs) from the metabolic network of the organism[35]. It may be noted that elementary modes contain the external metabolites with respective stoichiometric coefficients. Internal metabolites do not appear in elementary modes as they are balanced under the pseudo steady-state condition. Accumulation rates of extracellular metabolites can be represented in the term of fluxes of elementary modes and their corresponding stoichiometric coefficients. Mathematically, this relation can be written as following[31]:

$$A.x = b \qquad (1)$$

where, A is a matrix with each row containing stoichiometric coefficients of elementary modes for a particular external metabolite (Supplementary file 2, A-EMs). The vectors x and b represent fluxes of EMs and accumulation rates of extracellular metabolites, respectively. Here, x (fluxes of EMs) is an unknown column vector, which is to be calculated while b can be determined experimentally. Vector x can, thereafter, be computed using equation (1). Biological systems are, however, underdetermined and therefore, linear optimization was used to determine the fluxes of EMs (vector x) by maximizing or minimizing the yield of an external metabolite (e.g. biomass formation)[14, 20]. The corresponding linear programming problem can be formulated as:

$$Maximize \ a_i.x$$

$$Subject\ to \quad A'.x = b' \text{ and } 0 \leq x \leq \infty \qquad (2)$$

where, a_i stands for all the elements of ith row of matrix A or in other words, the accumulation rate of ith external metabolite used as an objective function. A' matrix and b' vector are obtained from A and b by removing the i^{th} row, corresponding to the extracellular metabolite.

The elements of the b' vector are experimentally determined quantities. However, measurements of all the external metabolites may not be experimentally feasible. In such a scenario, the rows corresponding to the non-measured metabolites form A' matrix and b' vector can be eliminated and thereafter, the vector x can be evaluated using linear

optimization technique as stated above (Supplementary file 2, A-EMs) . Equation 2 was solved using "linprog" in Matlab to obtain the unknown vector x (fluxes of elementary modes, using accumulation rate of a specific external metabolite as an objective function). For example, column vector b', contains accumulation rates of seven (glucose, biomass, acetic acid, butyric acid, acetone, butanol, and ethanol) out of total ten extracellular metabolites (glucose, biomass, acetic acid, butyric acid, acetone, butanol, ethanol, hydrogen, carbon dioxide, and water). The accumulation rates were used from a previous experimental study and used to perform elementary mode analysis on metabolic network in *C. acetobutylicum*[38]. The rows of external metabolites namely hydrogen, carbon dioxide and water (Supplementary file 2, A-EMs), were omitted from the analysis. Matrix A has rank seven, which suggests that at least seven independent measurements of accumulation rates of external metabolites would be required to satisfy carbon molar balance. Hence, use of seven out of the ten measurements completely describes the system (analysis not shown).

Flux distribution in the metabolic network (quantification of all biochemical reactions, Supplementary file 1, Table S2) of a given organism can be evaluated using matrix of elementary modes, EM, given that the flux vector of elementary modes is known. Rows of the matrix EM indicate the all biochemical reactions (both internal and exchange reactions); columns denote the flux of the elementary modes (Supplementary file 2, EM Reaction), and elements of the EM matrix are the corresponding stoichiometric coefficients. Exchange reactions are meant for reactions involved in transporting the external metabolites. YANAsquare software stores the EM matrix in memory during generation of elementary modes for a given set of biochemical reactions of an organism. Thus, flux distribution in the metabolic network (f) can be evaluated using matrix *EM* and the flux vector of elementary modes x, using the following equation:

$$EM.x = f \qquad (3)$$

In this work, matrix *EM* comprises of 42 biochemical reactions (Supplementary file 1, Table S2) and 67 elementary modes (Supplementary file 1, Table S3); and hence, has dimensions of 42×67. Moreover, f represents the column vector of 42 elements containing the fluxes of the biochemical reactions of the *C. acetobutylicum* metabolic network (Supplementary file 2, EM Reaction).

However, this linear system is an underdetermined system which generates more than one optimal solution. To handle this problem, two constraints – (i) molar balance among accumulation rates of external metabolites and (ii) steady state constraint for internal metabolites were used to calculate a unique flux distribution among reactions in original network under specific growth conditions. To address this issue further, we also performed Flux Variability Analysis (FVA) to get the extreme (maximum and minimum) values of each flux in the metabolic network. This was done as per the methodology described in Mahadevan and Schilling (2003)[39]. Using FVA, we calculate the maximum and minimum flux values of each reaction/elementary mode. The variability in flux values is highlighted in Supplementary file 1, Figure 4S. From our analysis, we note that in different possible solution sets, only 14 of the 67 fluxes showed a change in their values (data for Figure 4S in Supplementary file 3). The remaining 53 fluxes are invariant in our system. In addition, the only changes in the flux variability are quantitative in nature. There are no reactions or EMs, which changes from an OFF (flux equal to zero) to an ON state (flux greater than zero) across the optimal solution space. Hence, our analysis is able to predict the specific EMs/reaction in the ON or OFF state under a given condition.

Experimental Data Used

All experimental data used in this study for EM analysis is from a previous report published from our group[38]. All experimental procedures are described in detail in the text of the reference. Elemental composition of biomass used in this study was determined through measurement of carbon, hydrogen, nitrogen, and oxygen by CHNO Analyzer equipped with thermal conductivity detector (FLASH EA 1112 Series, Thermo Finnigan, Italy). Batch fermentation run was conducted in 5L fermentor with working volume of 2L using *C. acetobutylicum* to obtain biomass samples for elemental analysis. Fermentation samples were collected at two time points (20h and 40h) followed by centrifuged (at 10,000 rpm for 10 min),washed (three times with sterilized double distilled water), and dried. Dried biomass sample in powder form was used in CHNO Analyzer. An average of element percentage at both points for each component was employed to obtain final biomass molecular formula.

Metabolic network used for elementary mode analysis

The overall metabolic network of the organism is as shown in Figure 1. The biphasic central metabolic pathway of the bacterium comprises of a total of 51 metabolites in 42 biochemical reactions. Ten metabolites (biomass, acetic acid, butyric acid, acetone, butanol, ethanol, hydrogen, carbon dioxide, water, and glucose) were considered as extracellular metabolites and remaining 41 metabolites were intracellular metabolites. YANAsquare, a METATOOL integrated software tool, was used to generate elementary modes (EMs) from the set of reactions (Table S2 in Supplementary file 1). Biochemical reactions involved in central metabolism of *C. acetobutylicum* were obtained from literature based on KEGG database[15,36,16,17,37]. Redox balancing reactions (coupled with ferredoxin) catalyzed by ferredoxin: NAD(P)H oxidoreductase in hydrogen producing pathway was not annotated in KEGG, hence, the reaction was fixed as an irreversible reaction as previously reported in literature (for detail see previous section) (Table S2 in Supplementary file 1). However, we tested the possibility of the reaction to be reversible by assigning this reaction to be reversible in network analysis. The resulting topology was not found to realize experimental evidence of producing both acids (acetic and butyric acid) along with biomass formation over the consumption of glucose (results not shown). Since this was achieved assuming redox balancing reactions to be irreversible, this suggests that the only possible reduction of NAD^+ is via coupling with oxidation of ferredoxin in hydrogen producing pathway to maintain carbon flow.

Transport of glucose to inside the cell takes place through the phosphoenolpyruvate (PEP)-dependent phosphotransferase system (PTS) in the presence of soluble and membrane components[40]. PTS catalyzes uptake and phosphorylation of glucose simultaneously. Conversion of glucose to pyruvate through glycolytic pathway is connected with pentose phosphate pathway (PPP). Recently, in two parallel studies, PPP was characterized in *C. acetobutylicum*'s metabolic pathway by ^{13}C-based isotopomer analysis[19,18]. These reports revealed that oxidative reactions were absent in PPP, which is responsible for conversion of glucose-6-phosphate to ribulose-5-phosphate associated with NADPH and carbon dioxide synthesis in various organisms. Therefore, we did not consider the oxidative reactions in network for elementary mode analysis and connectivity between glycolysis and PPP was incorporated as sole activity of transketolase and transaldolase (Figure 1).

Moreover, hydrogen producing pathway is linked with pyruvate to acetyl-CoA conversion, and is a crucial pathway in terms of controlling electron and carbon flow. Ferredoxin: NAD(P)H oxidoreductase and hydrogenase are the key enzymes of this redox-balancing pathway, which are involved in oxidation of ferredoxin coupled with reduction of $NAD(P)^+$ and hydrogen production respectively (Figure 1)[41]. Ferredoxin: NAD(P)H oxidoreductase is not annotated in genome databases[36,15], although it is strongly hypothesized to be playing a role in controlling the electron and carbon flow[41]. In this direction, importance of reduction of $NADP^+$ to NADPH in redox balance reactions could be explained as an alternative pathway for NADPH production in PPP (oxidative pathway), which was found absent[18]. This hypothesis is considered in metabolic network analysis and reactions involved in oxidation of ferredoxin coupled with reduction of $NAD(P)^+$ were assigned to be irreversible[15]. In acidogenesis, ATP for growth is supplied from glycolysis and acids (acetic acid and butyric acid) producing pathway. It should be noted that butyric acid synthesis pathway is coupled with ATP formation and conversion of NAD^+ from NADH, while acetic acid synthesis is coupled with only ATP formation (Figure 1). Therefore, the strategy controlling the ratio of acetic and butyric acids likely lies on the balancing of ATP/ATP and NAD^+/NADH within the cell[41]. In solventogenesis, dehydrogenation reactions, which are involved in conversion of acetyl-CoA to ethanol and butyryl-CoA to butanol are NADH-dependent, while production of acetone is dependent on re-assimilation of acetic and butyric acid (Figure 1). Acetic acid has two pathways to be consumed; one is coupled with acetone production and second through reversible reactions of its production. Butyrate can be utilized only through one pathway which is coupled with acetone synthesis (the reactions involving butyric acid are irreversible)[15].

Biomass with molecular formula ($C_1H_{1.98}O_{0.50}N_{0.2}$) was considered an external metabolite in our analysis. For biomass formation, ribulose-5-phosphate, glycerate-1, 3-diphosphate, phosphoenolpyruvate, pyruvate, and acetyl-CoA associated with energy equivalents such as NADH, NADPH, and ATP was taken in account as precursors (Supplementary file 1). Moreover, carbon flow towards biomass formation from amino acids through citric acid cycle was balanced by stoichiometry of precursors of citric acid cycle like pyruvate and acetyl-CoA without including detailed reactions of citric acid cycle[18,19].

Results and Discussion

Elementary Modes (EMs) in the metabolic network of *C. acetobutylicum*

Based on our understanding of *Clostridium* metabolism as described in the methods section, a total of 67 elementary modes were obtained for further analysis (Figure S1 and Table S3 in Supplementary file 1). For analysis, we categorized the 67 EMs in three groups, Group 1 (5 EMs), Group 2 (23 EMs), and Group 3 (39 EMs), based on the direction of carbon flow and end products observed in each. Group 1 EMs comprise of those which use glucose as substrate and give biomass, acetic acid, and butyric acid as products. Group 2 EMs are responsible for solventogenesis. These use glucose, acetic acid, butyric acid as substrates; and produce acetone, butanol, and ethanol. There is no biomass formation in any of the group 2 EMs. The Group 3 EMs include fluxes which involve use of glucose as substrate, and production of biomass, acetic acid, butyric acid, acetone, butanol, and ethanol as products.

Group 1: Acidogenesis EMs

Out of a total of 67 EMs, Group 1 consists of five (EM1-EM5); these are involved exclusively with formation of biomass, acetic acid and butyric acid from consumption of glucose (Figure S1 and Table S3 in Supplementary file 1). Three EMs (EM1, EM2 and EM5) were associated with biomass synthesis coupled with butyric acid formation. All EMs in this group were linked with formation of butyric acid, which signifies that butyric acid synthesis in acidogenesis is essential. No pathway shows biomass formation coupled with only acetic acid. However, biomass synthesis associated with only butyric acid is possible as shown in EM1. The distribution of carbon flux between acetic acid and butyric acid is likely maintained by ratio of NADH and NAD^+ in redox balancing reaction of hydrogen producing pathway, which is catalyzed by ferredoxin: NAD(P)H oxidoreductase[41]. This analysis supports the hypothesis of presence of ferredoxin: NAD(P)H oxidoreductase in *C. acetobutylicum*'s central metabolic network, which is yet to be annotated experimentally[15]. Our analysis shows that growth of the organism is maximized in the acidogenesis phase when all carbon flux is processed through EM5.

Group 2: Solventogenesis EMs

A total of 23 EMs (EM6- EM28) are associated with formation of solvents (acetone, butanol, and/or ethanol) by consumption of glucose and/or acidogenesis products (Figure S1 and Table S3 in Supplementary file 1). Group 2

EMs specifically comprise those which utilize acids and glucose as substrates and convert them to solvents in the absence of growth. Interestingly, glucose was associated with all 23 EMs signifying that solventogenesis is only feasible while the media contains glucose. This behavior has been previously observed in a number of experimental reports, but not proposed explicitly as a constraint of solventogenesis[42–47]. No EM was found where either butyric or acetic acid served as sole carbon source, however, simultaneous utilization of individual/both acids along with glucose consumption is possible in solventogenesis (EM7, EM8, EM10, EM11, EM12, EM13, EM14, EM16, EM17, EM19, EM20, EM21, EM23, EM24, EM26, and EM28). Among Group 2 EMs, a total of 22 EMs were connected with acetone, while butanol and ethanol were linked with 15 and 8 EMs, respectively. Elementary mode analysis also revealed that synthesis of butanol or acetone is not feasible individually, but is rather coupled together in15 EMs. Further, formation of butanol is always coupled with acetone synthesis while acetone can be produced with either butanol or ethanol or both. Ethanol may be produced as the sole solvent through EM11. No pathway was detected for synthesis of individual solvent associated with hydrogen. Moreover, no pathway exists where all three solvents are formed simultaneously, indicating that solventogenesis is likely operated through a linear combination of a number of elementary modes. The precise objective function(s) employed by the cell in deciding this linear combination remains an open question.

Group 3: Acidogenesis and Solventogenesis EMs

This group consists of 39 EMs (EM29-EM67) with consumption and production patterns which cannot be classified as acidogenesis or solventogenesis only. A total of 10 EMs were involved in utilization of glucose and acetic acid simultaneously for synthesizing different combinations of products, such as: (i) biomass, acids and solvents (2 EMs), (ii) biomass and solvents (4 EMs) (iii) acids and solvents (4 EMs). Consumption of glucose and its combination with acetic acid or butyric acid, or with both acids was connected with 17 EMs producing biomass and solvents simultaneously. Moreover, simultaneous production of acids and solvents was detected in 12 EMs over the consumption of glucose and its combination with acetic acid. The EMs belonging to group 3 are of particular interest to us as they seem to exhibit features associated with both acidogenesis and solventogenesis. We speculate that these modes may also help shed light on unexplained phenotype of growth during solventogenesis associated with *C. acetobutylicum*[48,38,49].

Analysis of active Elementary Modes in "stressed" and "unstressed" acidogenesis and solventogenesis.

Quantification of fluxes in elementary modes was carried out by constraint based linear programming (Equation (2)) using accumulation rates from experimental data and the stoichiometric matrix, *S*, constructed from the 67 EMs in the metabolic network. Accumulation rates of seven extracellular metabolites (glucose, biomass, acetic acid, butyric acid, acetone, butanol, and ethanol) out of total ten extracellular metabolites were measured from experiments to establish molar balance for quantifying metabolic flux of elementary modes and individual reactions in network. As mentioned in the methods section, the flux values do not represent a quantitatively unique solution to the flux values. Our analysis shows that between the many solutions available, only 21 % fluxes show variability in their values. In addition, from a qualitative perspective, among the many solutions, there is no difference in the list of ON (EMs with non-zero flux values) and OFF EMs (EMs with flux equal to zero) in each experiment (data not shown). The data presented in the following sections refers to the condition of optimal growth. However, the results and analysis hold, if we were to choose any other solution consistent with our experimental data (data not shown).

All accumulation rates were expressed in mM h^{-1} and normalized with respect to glucose of 100 mM h^{-1}. This was done to investigate the flux distribution in the metabolic network under different growth conditions. Towards this end, we selected data from experiments with growth conditions as defined below:

(a) starting pH of 6.8, or 5.99, or 4.5 (and no control/external interference thereafter) [6.8 is the natural pH of the media prepared, *C. acetobutylicum* grows maximally at pH 6, and empirical evidence suggests that transition from acidogenesis to solventogenesis occurs at around a pH of 4.5);

(b) starting pH at 6.8 and not allowing the pH of the media to drop below 5.0 (upon the start of the experiment, the pH of the media drops because of acid formation. Once the pH reaches a value of 5.0, base was added to ensure that the pH value did not drop any further);

(c) starting pH of 4.5, and holding the pH at that value through the course of experiment;

(d) starting culture with 38 mmoles/L acetic acid, or 46 mmoles/L butyric acid (and no control/external interference thereafter); and

(e) starting with pH 5.99, and diluting with a supernatant of an identical culture after 20 hours of growth.

For our analysis, we classified these experimental conditions as "stressed" or "unstressed". Specifically, by "unstressed", we mean that once the experiment started, no external control was applied to regulate its pH or any quantity associated with the growth culture. However, “stressed” indicates that external reagents (stresses) were added to the media after the start of the fermentation. By this measure, we classify experiments (a) and (d) as "unstressed" conditions and experiments (b), (c), and (e) as "stressed" conditions. While in conditions (b) and (c), the external stress is applied as soon as acid formation starts, condition (e) is subjected to stress after 20 hours. The normalized accumulation rates, based on consumption of glucose at 100 mM/h, from each of the five conditions (during both, acidogenesis and solventogenesis) are presented in Table 1 (the raw values associated with each experiment are presented in Table S7 in Supplementary file 1).

To quantify the network, data was selected from two time-points for each experiment– one time point corresponded to maximal enzymatic activity during the exponential phase (during acidogenesis) and other time-point corresponds to early solventogenesis. Selected time points and their corresponding normalized values of accumulation rates for different fermentation experiments have been listed in Table 1. The data highlights two fundamental differences between the “stressed” and “unstressed” conditions. First, during the acidogenesis phase, there is no solvent production in the “unstressed” experiments, but both “stressed” experiments where pH is held constant exhibit solvent production. The “stressed” experiment (e) does not show any solvent production. But this is not surprising since in experiment (e), the external stress was only applied at the end of acidogenesis phase in the experiment. Secondly, during solventogenesis, the “unstressed” experiments exhibited consumption of acids without growth, whereas the “stressed” experiments exhibited either accumulation of acids and/or biomass production.

Flux distribution in network during acidogenesis under “stressed” and “unstressed” conditions

The normalized flux distribution of the network was almost identical while cells grew under different unstressed conditions. Similarly, under stress conditions, almost identical flux distribution was observed irrespective of the quality/quantity of stress (this flux distribution is distinct from the flux distribution in the unstressed conditions) (Table 1). Based on these results, an average flux distribution was evaluated for both unstressed and stressed (Figure 2(a) and 2(b)) states during exponential growth phase (or acidogenesis). Metabolic flux distribution in glycolytic pathway and biomass synthesis was almost unchanged irrespective of cells being in stressed or unstressed

conditions. Similarly, in both growth environments, the recently characterized PPP in *C. acetobutylicum*'s network was active to deliver the pentose sugars as a precursor for the formation of cellular components. Our analysis demonstrated that cells maintained similar ratio between fluxes of formation of acids in normal and stressed conditions (flux of extracellular butyric acid was around 40% higher than acetic acid). This was observed to be independent of the pH-stress even though under pH-stress, the organism activated additional pathways like those involved in acid consumption and solvent production. The fluxes of these additional pathways were zero at normal conditions. The net fluxes of extracellular acids were positive values (means acids were accumulated as extracellular metabolites) under stressed conditions. On the other hand, metabolic network of *C. acetobutylicum* contains enough flexibility in acidogenesis to cope with pH-stress without hampering its growth. These results suggest the robustness of the metabolic network to cope with variability in the environmental conditions, while growing at an optimal rate.

In hydrogen production pathway, flux of $NADP^+$ reduction was 92% and 62% higher than flux of NAD^+ reduction in normal and stressed conditions respectively(Figure 2(a) and 2(b)). This is because NADPH is required for biomass formation, which is active in both stressed and unstressed conditions during acidogenesis phase. Moreover, flux of NAD^+ reduction was 74.4% higher in stressed culture than in the case of normal conditions. This may be as a result of high requirement of NADH for NADH-dependent enzymes involved in ethanol (acetaldehyde dehydrogenase and alchohol dehydrogenase) and butanol (butyraldehyde dehydrogenase and butanol dehydrogenase[50]) production under stress conditions in acidogenesis, while in normal growth conditions NADH is required during the carbon flow towards butyric acid only. This illustrates that $NADH/NAD^+$ ratio is directly involved in regulating carbon flow in network. More precisely, pathway analysis postulated that this ratio induces alternative pathways towards solvent production for sustaining growth even during stressed environment. Flux of conversion of acetoacetate to acetone was exclusively dependent on (or coupled with) fluxes of reactions involved in intracellular assimilation of acids at all tested conditions.

Apart from pH-induced stress and unstressed growth conditions, we tested flux distribution on addition of acetic/butyric acid to the media (Tables 1)[38]. The idea behind this investigation was to identify the pathways which take part in regulating amount of acids inside the cell. Figure 3 represents the flux distribution in the network (acidogenesis) calculated from two separate experiments which were performed by addition of acetic acid and

butyric acid at the start of the fermentation experiment. The flux distribution in glycolytic pathway was invariant with respect to the effect of additional acids in media and there was no flux for reactions involved in solvent production, which suggests that solvent producing enzymes were not active on addition of either acids individually during acidogenesis. Most significantly, addition of acetic acid resulted in inactivity of enzymes responsible for acetic acid production (though we do not discount the likelihood of changes in expression levels of the enzyme). Moreover, addition of acetic acid did not affect biochemical reactions involved in butyric acid production.

Addition of butyric acid reduced the rate of reactions involved in butyric acid production (phosphotransbutyrylase, and butyrate kinase) by 30%, although the flux of reactions of acetic acid was unaffected. Similar effect was seen for the activity of ferredoxin: NADH oxidoreductase for reducing NAD^+ as indicated above ratio of NADH/NAD^+ affect carbon flow towards production of butyric acid. Addition of butyric acid also enhanced the flux of hydrogen evolution by 58%. This is likely due to the fact that redox reactions of ferredoxin are limited to carbon flow.

In spite of robustness of acid-producing pathways, assimilation of acids illustrates fragility of metabolism (details in next section). In general, network fragility implies that perturbation of even a single reaction can cause significant disruption of metabolic network. Additionally, flux of a reaction catalyzed by hydrogenase for hydrogen production was similar in acidogenesis under both stressed and unstressed conditions (Figure 2(a) and 2(b)). Similar values of flux at different growth conditions show the robustness of reaction. Overall, except activation of solvent-producing pathways under stresses conditions, our results suggest that pH-stress is unable to significantly alter the metabolic activity of the organism during acidogenesis phase. As mentioned before, these results emphasize the robustness of the metabolic network in its ability to sustain biomass production in the acidogenesis phase under a variety of stresses.

Flux distribution for solventogenesis in network under "stressed" and "unstressed" conditions

Unlike during acidogenesis, significant qualitative variation was observed in flux distribution patterns in solventogenesis phase between three uncontrolled fermentation experiments staring with a pH of 6.8, 5.99, and 4.5 (Figure 4(a) and Table 1). Comparative analysis of three unstressed conditions shows an invariant flux distribution in glycolytic pathway. Moreover, no carbon flow was observed in PPP as precursors synthesized from PPP were

connected to only biomass formation pathway, which was inactive during solventogenesis. Further, activity of Ferredoxin: NADPH oxidoreductase was absent because of absence of biomass synthesis. It should be noted that flux of NAD^+ reduction for oxidizing ferredoxin was 38% and 43% higher at initial pH 5.99 than 6.8 and 4.5 respectively. This was because fluxes of solvent producing reactions were higher at initial pH 5.99 and enzymes involved in solventogenesis are NADH-dependent. Therefore, solventogenesis phase required higher NADH pool. However, normalized flux of hydrogen evolution at initial pH 5.99 was two-fold lesser than in the case of pH 6.8 and 4.5 as protons pool moves towards reducing NAD^+ (Figure 1 and 4(a)). Remarkably, our analysis suggests that the distribution of fluxes between these two competitive reactions (reduction of NAD^+ and hydrogen evaluation) depends on the initial pH of the media. When fermentation started with an initial pH of 5.99, rapid accumulation of acids makes the pH drop to 4.5. At this pH, elementary mode analysis suggests low/no production of intracellular acids and high consumption of extracellular acids stimulates carbon flow towards solvent production. At the corresponding time in the experiments with starting pH of 6.8 and 4.5, the intermediate pH was below 4.0.

Solventogenesis phase also can be explained as survival strategy of the organism to consume and hence reduce the stress because of the acids. However, at initial uncontrolled pH level of 6.8 and 4.5, flux distribution postulated significant activity of acids producing enzymes simultaneously with consumption of acids. Notably, at initial pH 4.5 (intermediate pH below 4.0), acid (both, acetic and butyric) production and consumption in cell was carried out internally only (zero flux for consumption of extracellular acids). It shows that organism can maintain cyclic production and consumption of acids inside the cell for solvent production without consuming extracellular acids. On the other hand, metabolic network comprises alternative pathway for acids consumption when pathways for external acid consumption were not active. This coupling of acid consumption and solvent production or compulsion of acid consumption for solvent production shows a rigid node in the network. Specifically, extracellular and intracellular consumption of acetic acid can be carried out through two pathways – reversibly with production of acetic acid and irreversibly coupled with acetone production (Figure 1). On the basis of flux distribution, both these pathways are in operation together or individually in solventogenesis under unstressed and stressed conditions. Unlike acetic acid, consumption of butyric acid happens via a single pathway and is coupled with acetone production. Therefore, acetone production is dependent on enzymes involved in acetic and butyric acid consumption.

Different stressed conditions showed qualitatively similar flux distribution in network (solventogenesis). An average of normalized flux was determined and indicated in Figure 4(b). No significant difference in flux distribution was seen between acidogenesis (Figure 2(b)) and solventogenesis (Figure 4(b)) under stressed conditions except that activity of enzymes involved in $NADP^+$ reduction (ferredoxin-NADPH oxidoreductase), PPP (phosphopentoseisomerase, phosphopentoseepimerase, transketolase, transaldolase) was nil along with no biomass formation during solventogenesis. Under stressed conditions (constant pH levels), the bacterium demonstrated production of acids and solvents in both metabolic phases (acidogenesis and solventogenesis). Results of EMA illustrated that difference in flux distribution of biochemical reactions involved in acid and solvent production was not significant from one phase to another. Moreover, solventogenesis under stressed conditions showed 61% higher evolution of hydrogen than acidogenesis. This is because ferredoxin-NADPH oxidoreductase was not active here because of absence of biomass formation, so as competitive pathway, activity of hydogenase was high for evolving hydrogen to maintain the proton concentration balance across the cell membrane (proton motive force).Comparative analysis of metabolic flux distribution, in solventogenesis under stressed and unstressed conditions (Figure 4(a) and 4(b)) suggests that net fluxes are positive for consumption of extracellular acids simultaneous with solvent production (there was no consumption of extracellular acids) under stressed condition unlike unstressed conditions. It should be noted that in spite of zero consumption of external acids, pathways of internal acids consumption were active under stressed condition in acidogenesis and solventogenesis. This is also observed under normal growth conditions during solventogenesis. In summary, reversible reactions involved in acid production/consumption are associated with solvent production whether cells grow under unstressed or stressed growth conditions. It implies that perturbation in reactions involved in internal acids production may cause complete blockage of solvent producing pathways.

Figure 5 demonstrates the flux distribution in network during solventogenesis phase of a culture started with addition of butyric acid. It should be noted that solvents were not detectable during solventogenesis for the fermentation experiment with addition of acetic acid. Some variations were noteworthy in solventogenesis due to the addition of butyric acid to the culture. Owing to high amount of butyric acid in culture, flux of reactions of butyric acid production as well as reduction of NAD^+ was considerably reduced. Similarly, flux distribution from actoacetyl-CoA to butyryl-CoA was lower than what was found in other growth conditions. Therefore, butanol

production was dependent on consumption of extracellular butyric acid for carbon and on conversion of glyceraldehyde-3-phosphate to glyceraldehydes-1,3-diphosphate for NADH requirements. Slow rate of acetic acid producing reactions were detected. Moreover, biomass formation and associated PPP reactions were active, although the bacterium had entered solventogenesis.

Activation of group 3 Elementary Modes in "stress" conditions

Flux distribution in particular EMs was determined using experimental accumulation rates at selected time points in all experiments. In all unstressed experiment, only EMs of group 1 were active during acidogenesis. These EMs are associated with formation of acids and biomass. In these experiments, during solventogenesis, EMs of Group 1 and Group 3 were not functional and only EMs of Group 2 were in operation to produce solvents over the consumption of glucose and acids produced in acidogenesis. This switch in elementary modes quantitatively represents the qualitative shift in the behavior of the organism as it enters solventogenesis. Interestingly, no EM from Group 3 was activated in either of the metabolic phases under unstressed conditions (Figure 6).

Our analysis represents a qualitatively different behavior of the bacterium in stressed conditions. In these experiments, EMs from all three groups were found to be active simultaneously in metabolic network (during both acidogenesis and solventogenesis). The molar fluxes associated with each experiment during acidogenesis and solventogenesis are as shown in Figure 7. This demonstrates that the bacterium is able to modulate its cellular fluxes and invoke additional EMs in response to external stresses. Our quantitative flux distribution in unstressed and stressed conditions clearly demonstrates that there is a qualitative change in the behavior of the organism when external stress is imposed on the culture. We do not discount the possibility that external stresses create heterogeneity in the population with different fractions committed to acidogenesis and solventogenesis. We speculate that the additional EMs (whether invoked in a single cell, or arising in our analysis because of heterogeneity in our samples) act as a strategy employed by the bacterium to aid survival in presence of external stress. While the organism is prepared for tolerating the cellular stress imposed by its own fermentation, presence of external stress invokes additional EMs/heterogeneity in the organism.

Analysis of organism's strategies for consumption of substrates in solventogenesis

Elementary mode analysis was also employed to analyze organism's strategies for consuming three substrates (glucose, acetate, and butyric acid) in solventogenesis. Metabolites such as hydrogen, butanol, acetone and ethanol were selected as objective functions to find out the feasible phenotypic space or optimized solution space in metabolic network of *C. acetobutylicum*. Optimized solution space states that minimum to maximum range of substrates (glucose, acetic acid, and butyric acid) consumption rate simultaneously in solventogenesis for optimizing hydrogen, butanol, acetone, and ethanol individually. Constrained optimization by linear programming was used to maximize each objective function to investigate feasible contribution of substrates (glucose, acetic acid, and butyric acid) in solvent production. Glucose consumption rate was kept fixed as 100 mM h^{-1} and normalized consumption rates of acetic acid and butyric acid with respect to glucose was unbounded within the determined feasible ranges of 0-400 mM h^{-1} and 0-100 nM h^{-1}respectively.These feasible ranges demonstrate that organism would not consume the acetic acid and butyric acid more than the rate of 400 and 100 mM h^{-1}, respectively at fix glucose rate of 100 mM h^{-1} in solventogenesis. Feasible ranges of substrates were found to be equal for maximizing hydrogen, ethanol, acetone, and butanol individually. Above feasible ranges of acids and glucose consumption rate have been assigned in methodology to find out the maximum production rate of hydrogen, ethanol, acetone, or butanol.

Figure 8 shows the feasible solution space for accumulation rates of butanol, acetone, ethanol, and hydrogen with respect to normalized consumption rate of acetic acid and butyric acid. The maximum butanol accumulation rate was 140 mM h^{-1} corresponding consumption rates of glucose and butyric acid equal to 100 mM h^{-1}each and that of acetic acid in the range 80-320mM h^{-1}. Further, acetic acid consumption rate from 320-400 mM h^{-1} enforces increase in acetone production rate, while butanol production rate was decreased during this range of acetic acid. This may be because of carbon flow from glucose and acetic acid to acetone as acetic acid re-assimilation is coupled with acetone production. In contrast, butyric acid re-assimilation is also coupled with acetone production, although there are no biochemical reactions available for carbon flow from butyric acid to acetone. Our results show the butanol production is strongly dependent on butyric acid consumption, and at any given value of butyric acid consumption is independent of acetic acid consumption rate.

Similarly, other three objective functions (acetone, ethanol, and hydrogen) were maximized to find out optimized solution space for metabolites (Figure 9, and Figure S2 and S3 in Supplementary file 1). Maximum accumulation rates of acetone was obtained 300 mM h^{-1}on the acetic acid consumption rate of 400 mM h^{-1} and butyric acid consumption rate of 100mM h^{-1}(Figure 9). Optimizing yields of butanol or acetone leads no ethanol production. Synthesis rate of ethanol was highest (200 mM h^{-1}) for all the feasible consumption rates of acetic acid with no consumption of butyric acid (Figure S2 in Supplementary file 1). These results demonstrate that ethanol production is not dependent on butyric acid consumption in the metabolic network of *C. acetobutylicum*. Moreover, maximum hydrogen evolution rate of 200 mM h^{-1} was achieved at the entire feasible consumption rates of acetic acid and butyric acid (Figure S3 in Supplementary file 1). It means that hydrogen production is connected solely with glucose consumption pathway in network.

Calculation of maximum theoretical yield of metabolites

Last, we used EMA to determine of maximum theoretical yields of external metabolites and identification of concerned EMs is important to help optimize yield of target product(s). Therefore, maximum theoretical yield was calculated for various external metabolites from different carbon sources involved in acetone-butanol-ethanol (ABE) fermentation. Maximum theoretical yield of biomass on utilization of glucose alone was 0.85 moles per mole of glucose, which is associated with only EM5. Theoretical yield of acetic and butyric acid on glucose are 0.67 moles and 1 mole per mole of glucose respectively (EM4 for acetic acid and EM3 for butyric acid). Further, maximum theoretical yield of butanol is 0.47 moles on utilization of each mole of glucose, acetic acid, and butyric acid simultaneously, while butanol carried a yield of 0.8 mol mol^{-1} through two EMs (EM18 and EM25) utilizing glucose as only carbon source. Interestingly, these modes (EM18 and EM25) showed complete intracellular assimilation of both acids. Here, complete intracellular assimilation of acids indicates consumption of the acids produced and accumulated inside the cell (no secretion in surrounding media). Similarly, this topology of acids assimilation was seen during maximum theoretical yield of acetone on glucose (0.60 moles per mole of glucose). Additionally, elementary modes involved in maximum yield of butanol on glucose carried no production of hydrogen as the network uses hydrides for producing NADH in redox reaction, which is required for butanol production. In contrast, acetone production pathway does not require NADH and moves the network to produce hydrogen so as to maintain an optimum proton concentration in cytoplasm and pH gradient across the cell membrane[51].

514

515 Apart from butanol and acetone, ethanol carried a maximum theoretical yield of 2 moles per mole of glucose from
516 EM6, which showed production of ethanol as an individual solvent on glucose. However, none of ethanol producing
517 elementary modes was involved in production of ethanol via the consumption of butyric acid (alone or in
518 combination with glucose and acetic acid). In addition, the maximum theoretical yield of hydrogen was found to be
519 2 moles and 1 mole on glucose alone and on the combination of glucose, acetic acid and butyric acid, respectively.

520

521

Conclusions

In this work, we have analyzed the metabolic network of the bacterium *C. acetobutylicum* using elementary modes under a variety of environmental conditions. Experimental evidence regarding dynamics of *C. acetobutylicum* growth is conflicting, with some reports claiming that solventogenesis does not support growth[5,6], while others demonstrating growth in solventogenesis[38,48]. Our analysis demonstrates that depending on the EMs active at a particular time, the bacterium may/may not exhibit growth during the solventogenesis phase of metabolism. Further, our analysis shows that growth during solventogenesis is triggered by environmental stresses. This is done by invoking EMs which couple solventogenesis and biomass formation. Interestingly, in the absence of external stress, these EMs are in the OFF state (fluxes equal to zero) in all conditions tested in this study. Growth during stress conditions is likely a strategy to maximize the chances of survival when conditions are not ideal. Stress has also been reported to enhance gene expression of genes responsible for sporulation (and induce spore formation), again, increasing the chances of survival during harsh conditions[6]. An open question remains that why are these additional EMs not activated during unstressed conditions? Perhaps the internal mechanisms of the bacterium enable it to counter the stress generated in undisturbed conditions, and the additional EMs are only invoked at the time of an external stress (as against the one generated by its own acid production). The precise cue that triggers these EMs remains a focus of our future studies. In addition, the response of the cell at a single-cell resolution is another open ended question. It is quite likely that the bacterium prefers to split the population into heterogeneous groups, in order to maximize chances of survival.

Our analysis also highlights some of the subtle features of the network. Pathways involved in butyric acid production were active during all the stressed and unstressed conditions. The resulting butyric acid was either transported out of the cell or consumed inside the cell. These pathways can be considered as rigid nodes in the network. Production of acetic acid was controlled by its accumulation in media, while butyric acid has collective controlled mechanism by its accumulation in media and redox balance reactions of ferredoxin. Additionally, our analysis suggests that conversion of butyric acid to butyryl-CoA is likely a key step to control the production of butanol.

Acknowledgements

KG was funded by Department of Science & Technology (DST). SS was funded by the IYBA Program of Department of Biotechnology (DBT) and INPIRE Young Faculty Award (DST), Ministry of Science and Technology, Government of India.

References

1. S. Hu, H. Zheng, Y. Gu, J. Zhao, W. Zhang, Y. Yang, S. Wang, G. Zhao, S. Yang, and W. Jiang, *BMC Genomics*, 2011, **12**, 1–18.
2. M. Kumar and K. Gayen, *Appl. Energy*, 2011, **88**, 1999–2012.
3. C. L. Gabriel, *Ind. Eng. Chem.*, 1928, **20**, 1063–1067.
4. Y. Zhao, C. Tomas, F. B. Rudolph, E. Papoutsakis, and G. Bennett, *Appl. Environ. Microbiol.*, 2005, **71**, 530–537.
5. C. Grimmler, H. Janssen, D. Krausse, R.-J. Fischer, H. Bahl, P. Dürre, W. Liebl, and A. Ehrenreich, *J. Mol. Microbiol. Biotechnol.*, 2011, **20**, 1–15.
6. K. Alsaker and E. Papoutsakis, *J. Bacteriol.*, 2005, **187**, 7103–7118.
7. C. J. Paredes, K. V Alsaker, and E. T. Papoutsakis, *Nat. Rev. Microbiol.*, 2005, **3**, 969–78.
8. M. Kumar, Y. Goyal, A. Sarkar, and K. Gayen, *Appl. Energy*, 2012, **93**, 193–204.
9. B. A. Boghigian, H. Shi, K. Lee, and B. A. Pfeifer, *BMC Syst. Biol.*, 2010, **4**, 49.
10. K. Alsaker, T. Spitzer, and E. Papoutsakis, *J. Bacteriol.*, 2004, **186**, 1959–1971.
11. L. M. L. Harris, N. E. Welker, and E. E. T. Papoutsakis, *J. Bacteriol.*, 2002, **184**, 3586–3597.
12. J. Stelling, *Curr. Opin. Microbiol.*, 2004, **7**, 513–8.
13. B. P. Tracy, S. W. Jones, and E. T. Papoutsakis, *J. Bacteriol.*, 2011, **193**, 1414–26.
14. K. Gayen and K. V Venkatesh, *BMC Bioinformatics*, 2006, **7**, 445.
15. J. Lee, H. Yun, A. M. Feist, B. Ø. Palsson, and S. Y. Lee, *Appl. Microbiol. Biotechnol.*, 2008, **80**, 849–62.
16. R. S. Senger and E. T. Papoutsakis, *Biotechnol. Bioeng.*, 2008, **101**, 1036–52.
17. R. S. Senger and E. T. Papoutsakis, *Biotechnol. Bioeng.*, 2008, **101**, 1053–71.
18. D. Amador-Noguez, X.-J. Feng, J. Fan, N. Roquet, H. Rabitz, and J. D. Rabinowitz, *J. Bacteriol.*, 2010, **192**, 4452–61.
19. S. B. Crown, D. C. Indurthi, W. S. Ahn, J. Choi, E. T. Papoutsakis, and M. R. Antoniewicz, *Biotechnol. J.*, 2011, **6**, 300–5.
20. K. Gayen, M. Gupta, and K. V Venkatesh, *In Silico Biol.*, 2007, **7**, 123–39.
21. L. F. de Figueiredo, A. Podhorski, A. Rubio, C. Kaleta, J. E. Beasley, S. Schuster, and F. J. Planes, *Bioinformatics*, 2009, **25**, 3158–65.
22. G. Beuster, K. Zarse, C. Kaleta, R. Thierbach, M. Kiehntopf, P. Steinberg, S. Schuster, and M. Ristow, *J. Biol. Chem.*, 2011, **286**, 22323–30.

23. J. Zirkel, A. Cecil, F. Schäfer, S. Rahlfs, A. Ouedraogo, K. Xiao, S. Sawadogo, B. Coulibaly, K. Becker, and T. Dandekar, *Bioinform. Biol. Insights*, 2012, **6**, 287–302.

24. C. Liang, M. Liebeke, R. Schwarz, D. Zühlke, S. Fuchs, L. Menschner, S. Engelmann, C. Wolz, S. Jaglitz, J. Bernhardt, M. Hecker, M. Lalk, and T. Dandekar, *Proteomics*, 2011, **11**, 1915–35.

25. J. Reed and B. Palsson, *J. Bacteriol.*, 2003, **185**, 2692–2699.

26. I. Thiele, A. Heinken, and R. Fleming, *Curr. Opin. Biotechnol.*, 2012, **24**, 1–9.

27. J. Stelling, S. Klamt, K. Bettenbrock, S. Schuster, and E. D. Gilles, *Nature*, 2002, **420**, 190–3.

28. S. Schuster, T. Dandekar, and D. A. Fell, *Trends Biotechnol.*, 1999, **17**, 53–60.

29. S. Klamt and J. Stelling, *Trends Biotechnol.*, 2003, **21**, 64–9.

30. C. T. Trinh, A. Wlaschin, and F. Srienc, *Appl. Microbiol. Biotechnol.*, 2009, **81**, 813–26.

31. S. Schuster and C. Higetag, *J. Biol. Syst.*, 1994, **2**, 165–182.

32. S. Schuster, D. A. Fell, and T. Dandekar, *Nat. Biotechnol.*, 2000, **18**, 326–32.

33. S. Klamt, J. Saez-Rodriguez, and E. Gilles, *BMC Syst. Biol.*, 2007.

34. R. Schwarz, P. Musch, A. von Kamp, B. Engels, H. Schirmer, S. Schuster, and T. Dandekar, *BMC Bioinformatics*, 2005, **6**, 135.

35. R. Schwarz, C. Liang, C. Kaleta, M. Kühnel, E. Hoffmann, S. Kuznetsov, M. Hecker, G. Griffiths, S. Schuster, and T. Dandekar, *BMC Bioinformatics*, 2007, **8**, 313.

36. C. B. Milne, J. A. Eddy, R. Raju, S. Ardekani, P.-J. Kim, R. S. Senger, Y.-S. Jin, H. P. Blaschek, and N. D. Price, *BMC Syst. Biol.*, 2011, **5**, 130.

37. M. Kanehisa, S. Goto, M. Hattori, K. F. Aoki-Kinoshita, M. Itoh, S. Kawashima, T. Katayama, M. Araki, and M. Hirakawa, *Nucleic Acids Res.*, 2006, **34**, D354–7.

38. M. Kumar, K. Gayen, and S. Saini, *Bioresour. Technol.*, 2013, **138**, 55–62.

39. R. Mahadevan and C. H. Schilling, *Metab. Eng.*, 2003, **5**, 264–276.

40. M. Tangney and W. J. Mitchell, *Appl. Microbiol. Biotechnol.*, 2007, **74**, 398–405.

41. D. T. Jones and D. R. Woods, *Microbiol. Rev.*, 1986, **50**, 484–524.

42. F. Monot, J. R. Martin, H. Petitdemange, and R. Gay, *Appl. Environ. Microbiol.*, 1982, **44**, 1318–24.

43. P. J. Evans and H. Y. Wang, *Appl. Environ. Microbiol.*, 1988, **54**, 1662–7.

44. R. A. Holt, G. M. Stephens, and J. G. Morris, *Appl. Environ. Microbiol.*, 1984, **48**, 1166–1170.

45. Y. Jiang, C. Xu, F. Dong, Y. Yang, W. Jiang, and S. Yang, *Metab. Eng.*, 2009, **11**, 284–91.

46. J. W. Roos, J. K. McLaughlin, and E. T. Papoutsakis, *Biotechnol. Bioeng.*, 1985, **27**, 681–94.

47. R. P. Desai, L. M. Harris, N. E. Welker, and E. T. Papoutsakis, *Metab. Eng.*, 1999, **1**, 206–13.

48. X. Yang, M. Tu, R. Xie, S. Adhikari, and Z. Tong, *AMB Express*, 2013, **3**, 3.

49. Z. Sun and S. Liu, *Biomass and Bioenergy*, 2010, 1–9.

50. G. Rajagopalan, J. He, and K.-L. Yang, *BioEnergy Res.*, 2013, **6**, 240–251.

51. R. Gheshlaghi, J. M. Scharer, M. Moo-Young, and C. P. Chou, *Biotechnol. Adv.*, 2009, **27**, 764–81.

Figure captions

Figure 1 Schematic diagram of *C. acetobutylicum* metabolic network. Dotted box indicates cell membrane. Metabolic reactions are indicated using arrows. Arrows which cross the cell membrane are transport reactions indicating transfer of external metabolites.

Figure 2 Flux distribution during acidogenesis in *C. acetobutylicum* metabolic network under unstressed and stressed conditions. **(a)** Average flux values in uncontrolled fermentation experiments with starting pH as 6.8, 5.99, and 4.5. **(b)** Average flux values in a fermentation with starting pH as 6.8 and holding it thereafter at 5.0, and another experiment with a constant pH of 4.5. Fluxes/rates of reactions were determined in mM h^{-1}. Fluxes with negative sign indicate that the reaction is proceeding in a direction indicated by gray arrows. All abbreviations are expanded in Table S1 in the Supplement.

Figure 3 Flux distribution during acidogenesis in *C. acetobutylicum* metabolic network for the fermentations, which were started with addition of acetic or butyric acid. The two numbers against each reaction (arrow) indicate the flux corresponding to experiment with prior addition of acetic acid (top number) or butyric acid (bottom number). Fluxes/rates of reactions were determined in mM h^{-1}. Fluxes with negative sign indicate that the reaction is proceeding in a direction indicated by gray arrows. All abbreviations are expanded in Table S1 in the Supplement.

Figure 4 Flux distribution during solventogenesis in *C. acetobutylicum* metabolic network under unstressed and stressed conditions. **(a)** Flux values in fermentation experimentations done under uncontrolled pH 6.8, 5.99, and 4.5 (top, middle, and bottom respectively). **(b)** Average flux values fermentations under starting pH with 6.8 and holding it constant at 5.0 and experiment with a constant pH of 4.5. Fluxes/rates of reactions were determined in mM h^{-1}. Fluxes with negative sign indicate that the reaction is proceeding in a direction indicated by gray arrows. All abbreviations are expanded in Table S1 in the Supplement.

Figure 5 Flux distribution during solventogenesis in *C. acetobutylicum* metabolic network for fermentation experiment which was started with addition of butyric acid. Fluxes/rates of reactions were determined in mM h^{-1}.

Fluxes with negative sign indicate that the reaction is proceeding in a direction indicated by gray arrows. All abbreviations are expanded in Table S1 in the Supplement.

Figure 6 Flux distribution in individual elementary modes under various unstressed conditions **(a)** uncontrolled starting pH of 6.8 (acidogenesis and solventogenesis), **(b)** uncontrolled starting pH of 5.99 (acidogenesis and solventogenesis), **(c)** uncontrolled starting pH of 4.5 (acidogenesis and solventogenesis) **(d)** starting culture with 38 mmoles/L acetic acid (acidogenesis), and **(e)** starting culture with 46 mmoles/L butyric acid (acidogenesis and solventogenesis). Flux is expressed in mM h^{-1}. EM1-EM5, EM6-EM28, and EM 29-EM67 represent Group 1 , Group 2, and Group 3, respectively. Black and gray colors represent fluxes in acidogenesis and solventogenesis, respectively.

Figure 7 Flux distribution in elementary modes under stressed conditions. **(a)** and **(b)** starting pH at 6.8 and not allowing the pH of the media to drop below 5.0 (acidogenesis and solventogenesis, respectively), **(c)** and **(d)** starting pH of 4.5, and holding the pH at that value through the course of experiment (acidogenesis and solventogenesis, respectively), **(e)** and **(f)** starting with pH 5.99, and diluting with a supernatant of an identical culture after 20 hours of growth (acidogenesis and solventogenesis, respectively) **(d)** starting culture with 38 mmoles/L acetic acid (acidogenesis), and **(e)** starting culture with 46 mmoles/L butyric acid (acidogenesis and solventogenesis). Flux is expressed in mM h^{-1}. EM1-EM5, EM6-EM28, and EM 29-EM67 represent Group 1, Group 2, and Group 3, respectively. Black and gray colors represent fluxes in acidogenesis and solventogenesis, respectively.

Figure 8 Feasible solution spaces for butanol synthesis with respect to acetic acid and butyric acid consumption in *C. acetobutylicum*. Consumption rate of glucose was fixed (100 mM h^{-1}), and consumption rate of acetic acid and butyric acid were varied within the determined feasible range of 0-400 mM h^{-1} and 0-100 nM h^{-1} respectively. Butanol synthesis was considered as objective function to find optimized solution spaces.

Figure 9 Feasible solution spaces for acetone synthesis with respect to acetic acid and butyric acid consumption in *C. acetobutylicum*. Consumption rate of glucose was fixed (100 mM h^{-1}), and consumption rate of acetic acid and

butyric acid were varied within the determined feasible range of 0-400 mM h^{-1} and 0-100 nM h^{-1} respectively. Acetone synthesis was considered as objective function to find optimized solution spaces.

Table captions

Table 1 Normalized accumulation rates (mM h^{-1}) of external metabolites with respect to glucose (100 mM h^{-1}) during acidogenesis and solventogenesis in *C. acetobutylicum* under unstressed and unstressed conditions.

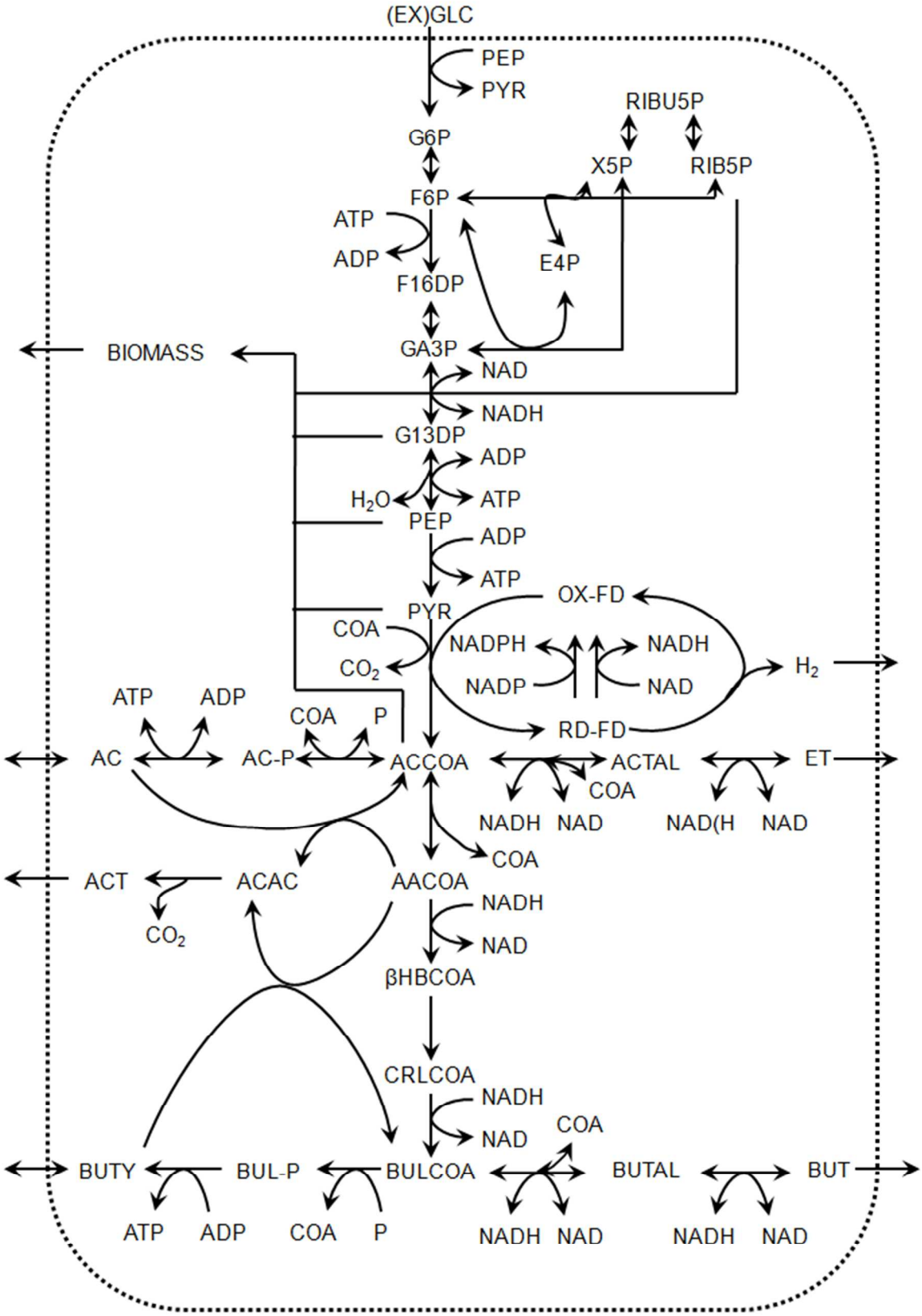

Figure 1

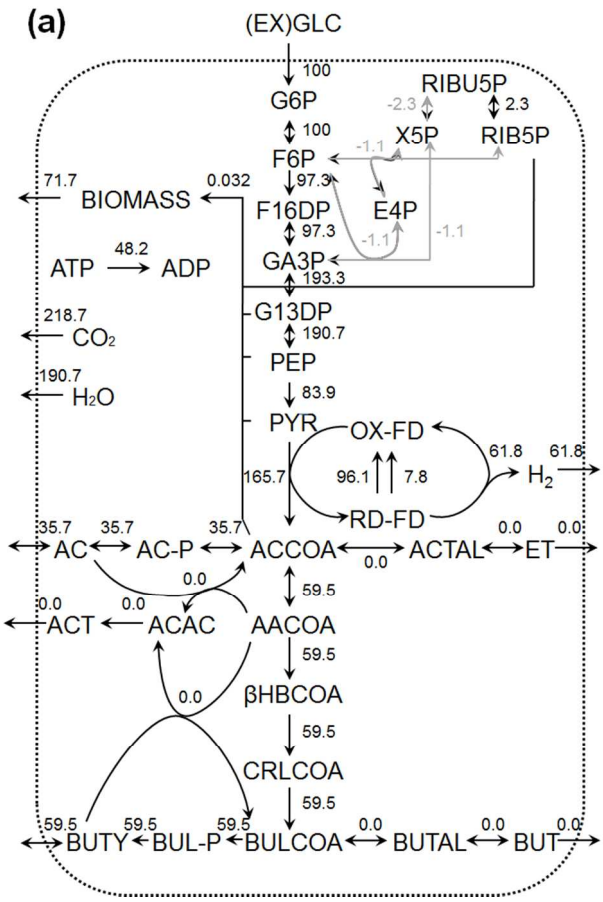

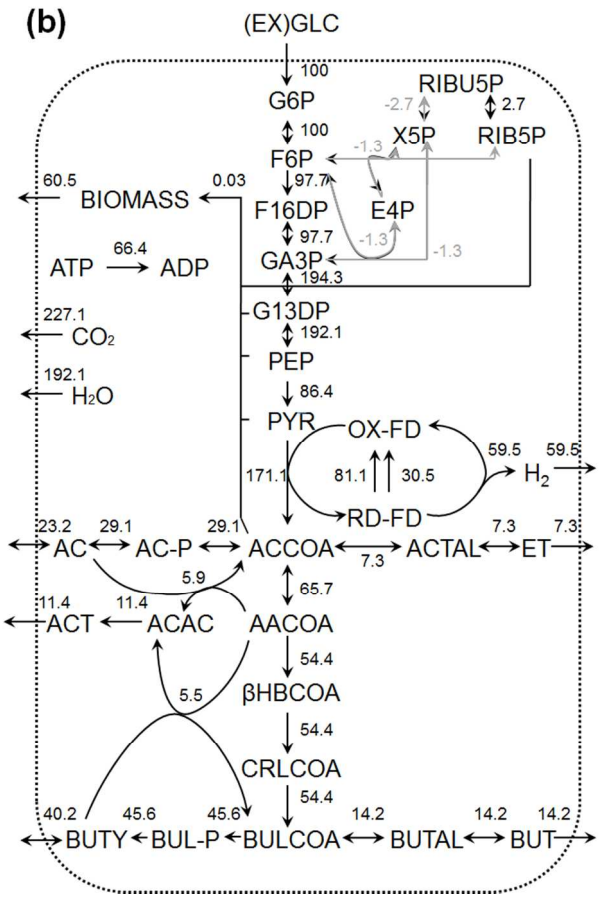

Figure 2

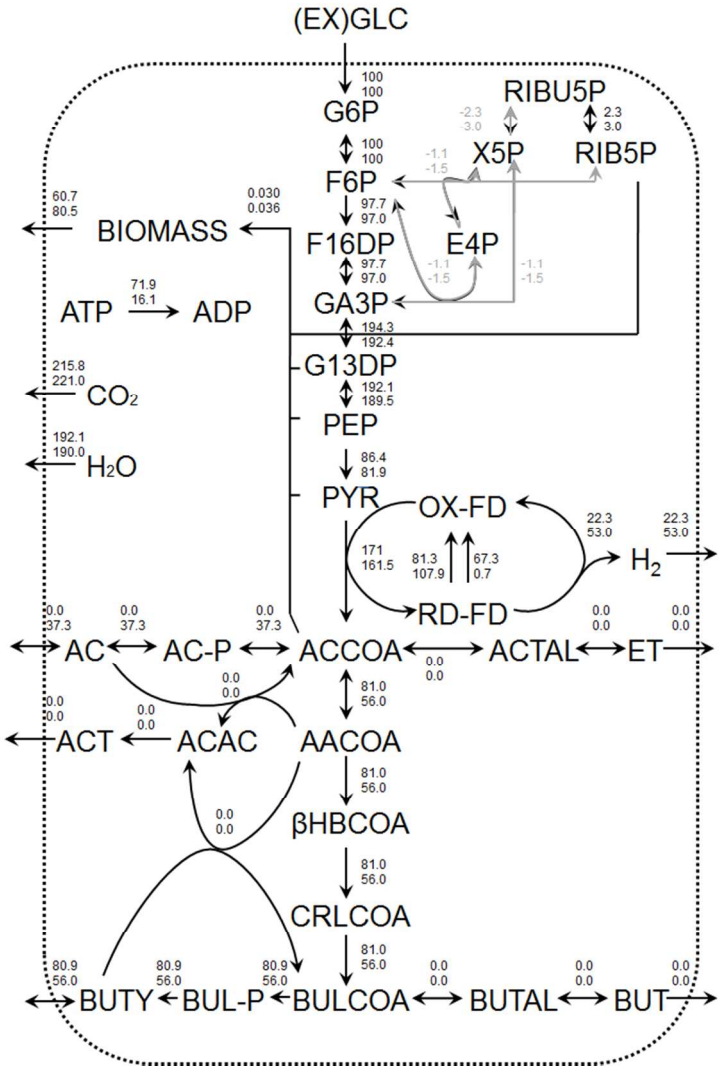

Figure 3

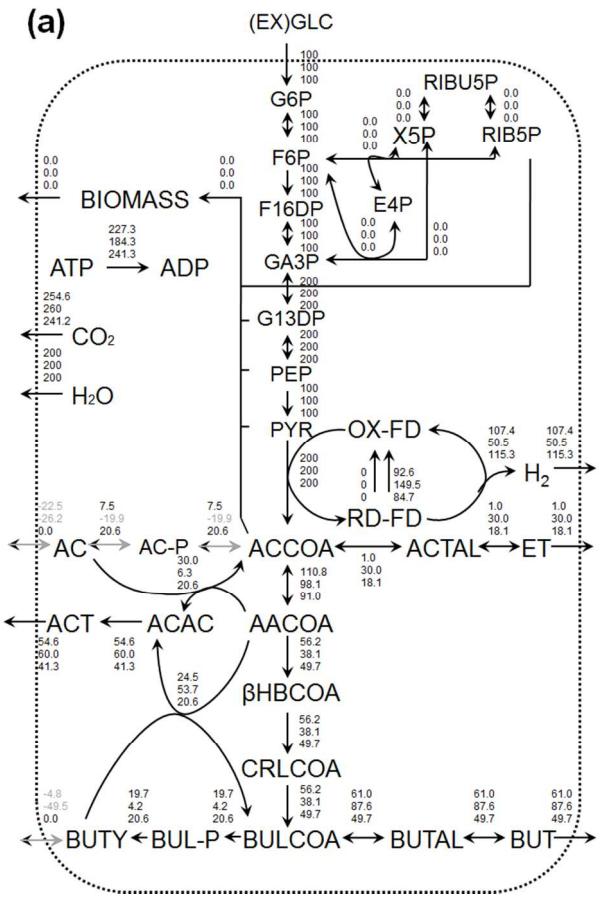

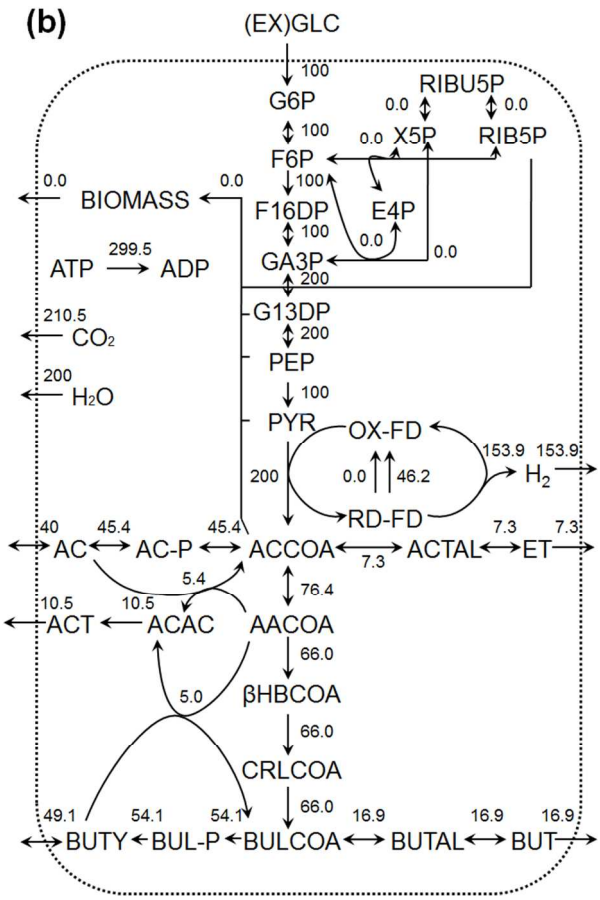

Figure 4

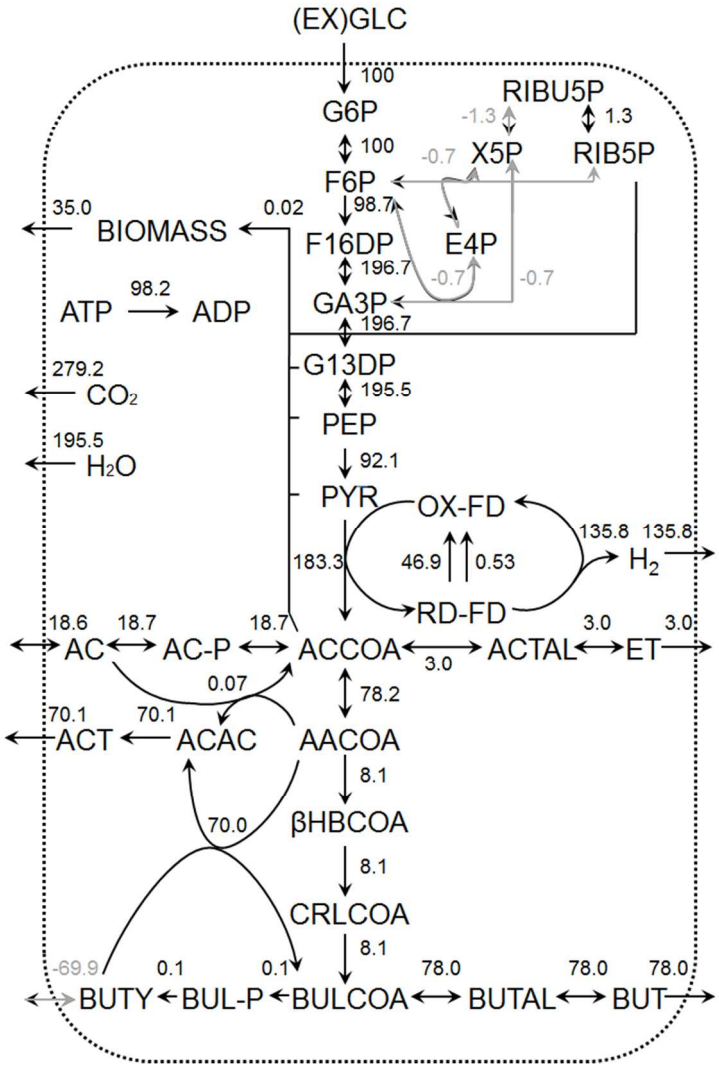

Figure 5

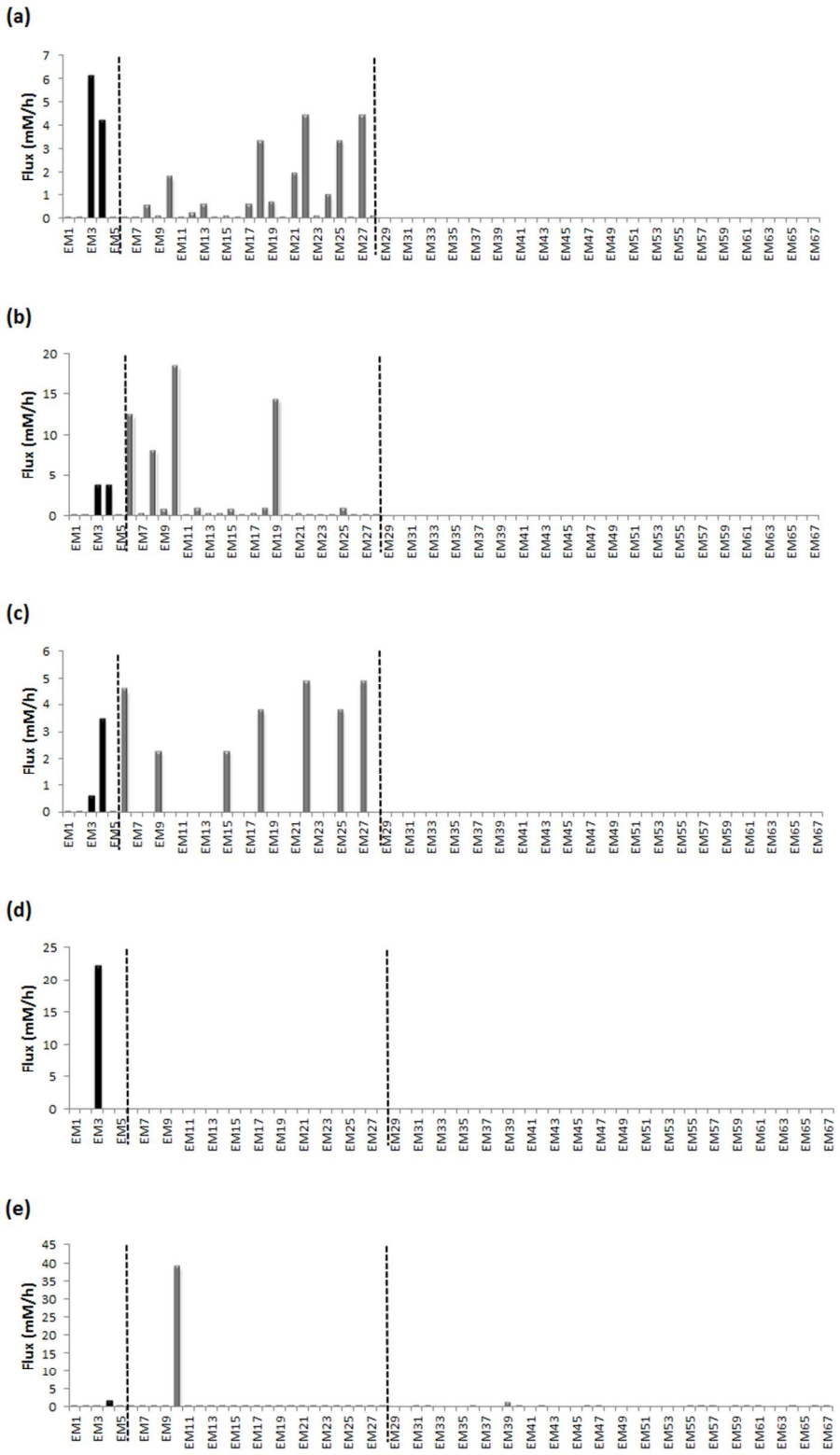

Figure 6

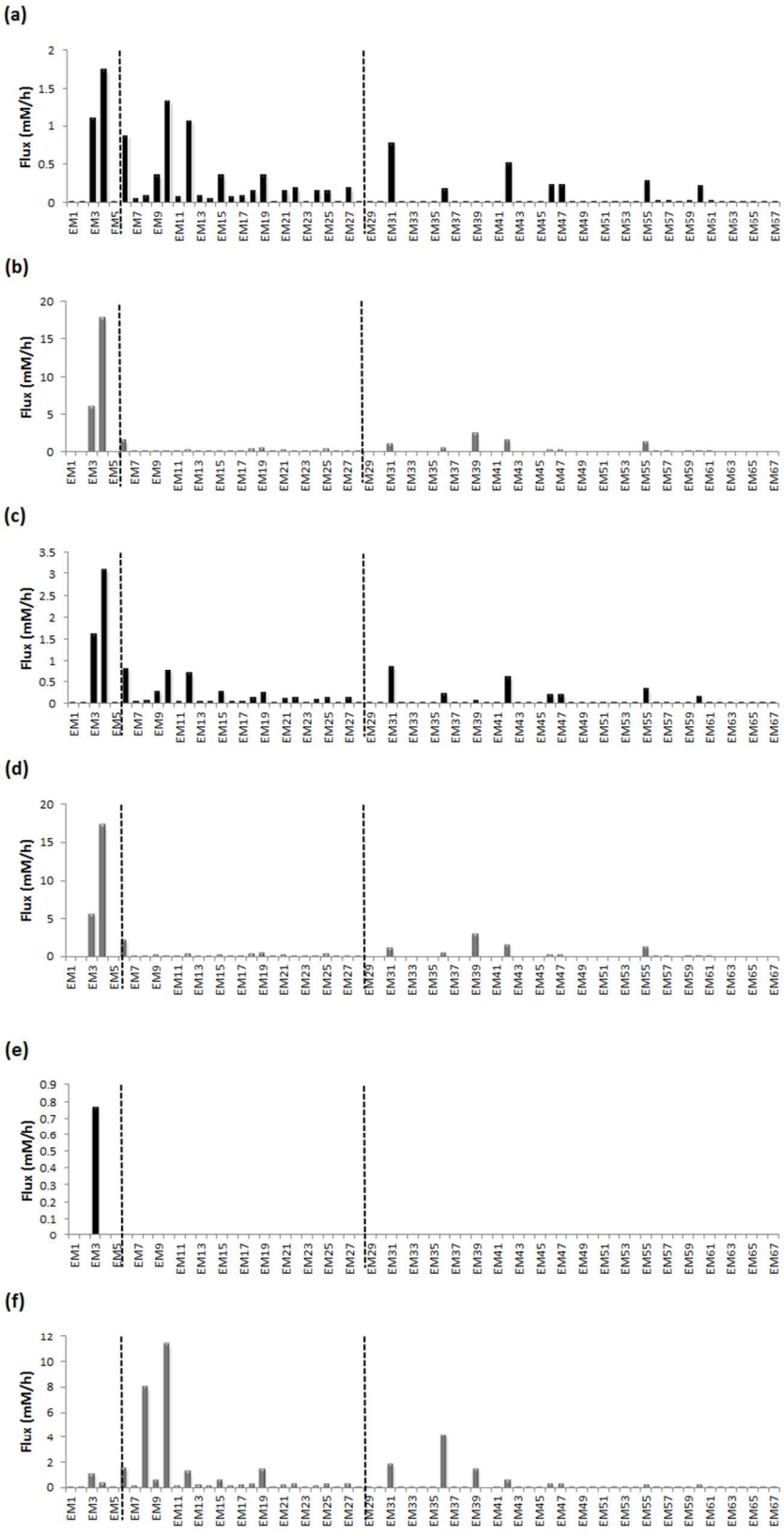

Figure 7

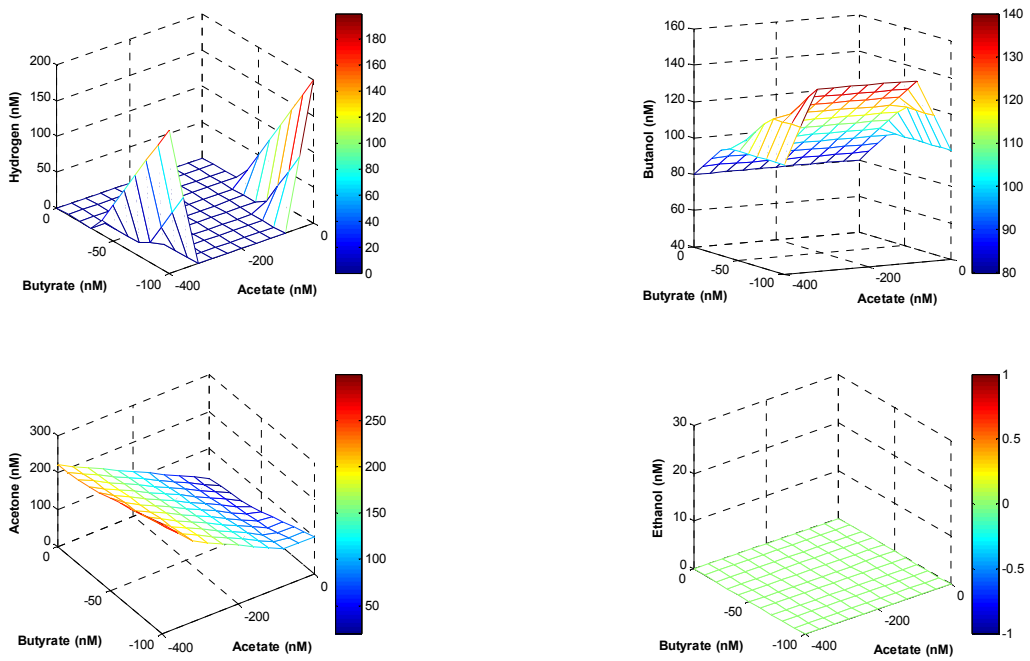

Figure 8

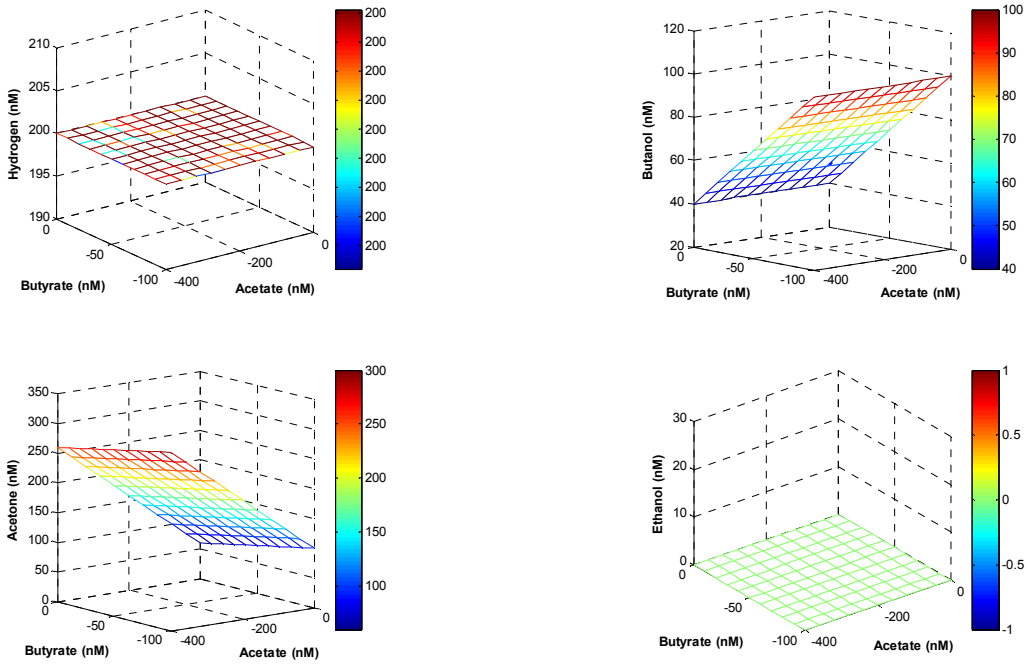

Figure 9

Table 1

Metabolic phase	External metabolites	Normalized accumulation rate with respect to glucose (100 mM h^{-1})							
		Unstressed conditions					Stressed conditions		
		Initial pH 6.8	Initial pH 5.99	Initial pH 4.5	Addition of acetic acid	Addition of butyric acid	Starting with 6.8 and holding at 5.0	Constant pH 4.5	Diluted culture
Acidogenesis	Glucose	-100	-100	-100	-100	-100	-100	-100	-100
	Biomass	68.4	71.8	75	60.7	80.5	61.0	60.0	83.8
	Acetic acid	34.9	35.5	36.7	0	37.3	27.5	28.9	35.0
	Butyric acid	60	59.6	58	80.9	56.0	40.0	40.3	56.1
	Acetone	-	-	-	-	-	9.0	8.7	-
	Butanol	-	-	-	-	-	14.5	13.9	-
	Ethanol	-	-	-	-	-	7.0	7.5	-
Solventogenesis	Glucose	-100	-100	-100	-100	-100	-100	-100	-100
	Biomass	-	-	-	-	35	-	-	14.4
	Acetic acid	-22.5	-26.2	0	-	18.6	40.0	39.9	-11.9
	Butyric acid	-4.8	-49.5	0	-	-69.9	50.3	47.8	-25.3
	Acetone	54.6	60	41	-	70.0	10.0	11.0	52.0
	Butanol	61	87.6	49.7	-	78.0	16.5	17.3	66.9
	Ethanol	1.0	30	18.1	-	3.0	6.5	8.0	15.7